Visual Neuroscience (1992), 9, 279-290. Printed in the USA.

A coupled network for parasol but not midget ganglion cells in the primate retina

DENNIS M. DACEY AND SARAH BRACE
Department of Biological Structure, University of Washington, Seattle
(RECEIVED October 28, 1991; ACCEPTED January 22, 1992)

Abstract

Intracellular injections of Neurobiotin were used to determine whether the major ganglion cell classes of the macaque monkey retina, the magnocellular-projecting parasol, and the parvocellular-projecting midget cells showed evidence of cellular coupling similar to that recently described for cat retinal ganglion cells. Ganglion cells were labeled with the fluorescent dye acridine orange in an *in vitro*, isolated retina preparation and were selectively targeted for intracellular injection under direct microscopic control. The macaque midget cells, like the beta cells of the cat's retina, showed no evidence of tracer coupling when injected with Neurobiotin. By contrast, Neurobiotin-filled parasol cells, like cat alpha cells, showed a distinct pattern of tracer coupling to each other (homotypic coupling) and to amacrine cells (heterotypic coupling).

In instances of homotypic coupling, the injected parasol cell was surrounded by a regular array of 3-6 neighboring parasol cells. The somata and proximal dendrites of these tracer-coupled cells were lightly labeled and appeared to costratify with the injected cell. Analysis of the nearest-neighbor distances for the parasol cell clusters showed that dendritic-field overlap remained constant as dendritic-field size increased from 100-400 μm in diameter.

At least two amacrine cell types showed tracer coupling to parasol cells. One amacrine type had a small soma and thin, sparsely branching dendrites that extended for 1-2 mm in the inner plexiform layer. A second amacrine type had a relatively large soma, thick main dendrites, and distinct, axon-like processes that extended for at least 2-3 mm in the inner plexiform layer. The main dendrites of the large amacrine cells were closely apposed to the dendrites of parasol cells and may be the site of Neurobiotin transfer between the two cell types. We suggest that the tracer coupling between neighboring parasol cells takes place indirectly *via* the dendrites of the large amacrine cells and provides a mechanism, absent in midget cells, for increasing parasol cell receptive-field size and luminance contrast sensitivity.

Keywords: Primate retina, Retinal ganglion cells, Magnocellular and parvocellular pathways, Tracer coupling

Introduction

In the primate retina the two major ganglion cell classes, the midget and parasol cells, are the origin of distinct, retinocortical visual pathways. The midget and parasol cells project, respectively, to the parvocellular and magnocellular layers of the dorsal lateral geniculate nucleus. Parvocellular-projecting cells have small dendritic and receptive fields, show tonic, color-opponent responses to light and make up the great majority of ganglion cells. Magnocellular-projecting cells have larger dendritic and receptive fields, show phasic, nonopponent light responses, and are 8-10 times more sensitive to luminance contrast than parvocellular-projecting cells (for review see Kaplan et al., 1990).

The great anatomical and physiological differences between the midget and parasol cells are likely to be related to equally significant differences in retinal wiring for the two cell classes, but it has been difficult to clearly identify presynaptic cone bipolar or amacrine cell types that are uniquely related to either parasol or midget cells. For cone bipolar cells, it has been suggested that the midget and parasol cells may receive selective input, respectively, from midget bipolar cells (presumed color-selective) and diffuse bipolar cell types (presumed noncolor selective) (Boycott & Wässle, 1991). A recent electron-microscopic study of synaptic inputs to human parafoveal midget cells supports this hypothesis (Kolb & Dekorver, 1991). Such a bipolar connectivity pattern would provide a simple explanation for the difference in color selectivity between the midget and parasol cells. Concerning amacrine cells, there is no evidence, either light or electron microscopic, for unique or shared connections of midget and parasol cells with any identified cell type.

One problem in understanding the retinal connections of the midget and parasol cells has been the lack of unique markers that distinguish different presynaptic cell types. Recently an intracellular marker has been introduced that has the potential for providing new information about retinal circuitry. Intracellu-

Reprint requests to: Dennis M. Dacey, Department of Biological Structure, SM-20, University of Washington, Seattle, WA 98195, USA.

lar injections of the biotin compounds, Neurobiotin or biocytin, have revealed tracer coupling among a wide variety of retinal cell types (Vaney, 1991). Neurobiotin fills of the two major ganglion cell classes of the cat's retina, the alpha Y and the beta X cells, showed tracer coupling between neighboring alpha cells (homotypic coupling) and between alpha cells and amacrine cells (heterotypic coupling) but, by contrast, no tracer coupling for beta cells.

In the present study, we used intracellular injections of Neurobiotin to look for tracer coupling in macaque parasol and midget cells. Arguments based primarily on anatomical evidence have suggested that the parasol and midget cells are the primate equivalents, respectively, of the cat alpha and beta cells (Leventhal et al., 1981; Rodieck et al., 1985). However, species differences in some of the physiological properties of these cells have also suggested that parasol cells are equivalent to beta cells, while midget cells have no homologue in the cat, and alpha cells have no identified homologue in primate (Shapley & Perry, 1986; Silveira & Perry, 1991). Here we show that the parasol cells have a pattern of both homotypic and heterotypic coupling that appears identical to that described for the cat alpha cells using the same technique. By contrast the midget cells, like the cat beta cells, show no evidence of tracer coupling.

An analysis of the pattern of intracellular staining in the macaque showed that at least two morphologically distinct amacrine cell types were coupled to the parasol cells. The detailed morphology of the amacrine cells further indicated that the tracer coupling between neighboring parasol cells may take place indirectly, *via* these amacrine cells. The distinct morphology of the amacrine cell processes also suggested that they could contribute to formation of the parasol cell's receptive field.

While this paper was in preparation, an abstract appeared reporting that intracellular injection of Neurobiotin into parasol cells revealed tracer coupling between neighboring parasol cells and between parasol cells and amacrine cells with cell bodies in the ganglion cell layer (Rodieck & Haun, 1991).

Materials and methods

This study is based on results from *Macaca nemestrina* retinas ($n = 24$) obtained from the Tissue Program of the Regional Primate Center at the University of Washington. Experiments were also done on a single baboon (*Papio c. anubis*) retina; the results were indistinguishable from the macaque. Methods for isolation and maintenance of the retina *in vitro* and for intracellular injection of retinal cells have been reported previously (Dacey, 1989*a*,*b*; 1990*b*).

In brief, retinas were first dissected free of the vitreous humor and eyecup in oxygenated culture medium (Ames; Sigma, St. Louis, MO) and then placed flat, vitreal side side up, in a chamber on the stage of a light microscope and continuously superfused with oxygenated medium. Retinal cells were vitally stained by adding a few drops of the fluorescent dye acridine orange (~1 mM solution) to the superfusate as it entered the chamber. Fine-tipped, low-resistance intracellular microelectrodes were formed from thin-walled microcapillary glass on a Brown-Flaming micropipette puller and filled with a solution of 4% Neurobiotin (Vector Labs, Burlingame, CA) and 1–2% Lucifer Yellow (Aldrich, Milwaukee, WI) in MOPS buffer (Sigma, 20 mM, pH 7.6) to give an initial resistance of ~100 MΩ. The electrodes were beveled to a final resistance of 36–42 MΩ with a K.T. Brown beveler. The electrode tip and the retina were viewed together under epifluorescence illumination at high resolution with a Zeiss 40× water-immersion, long-working distance objective.

Both Lucifer Yellow fluorescence in the microelectrode and the acridine fluorescence of ganglion cell somata were observed with the same filter combination (excitation filter, 410–490 nm; barrier filter, 515 nm). Cell penetration was confirmed by iontophoresis of Lucifer Yellow into the cell (0.1–1.0 nA, negative current, for 5–10 s). If the penetration was successful the cell was then injected with Neurobiotin (1–2 nA, positive current, for 1–3 min). Retinas were removed from the superfusion chamber after ~6 h and fixed in phosphate-buffered 4% paraformaldehyde (0.1 M; pH 7.4) for ~2 h. The intracellular Neurobiotin was revealed by a horseradish peroxidase (HRP) reaction product using the Vector ABC protocol (Vector, Elite kit) to bind the Neurobiotin to HRP as follows. Retinas were placed in 0.5% triton X-100 (in 0.1 M phosphate buffer) at room temperature for 3 h, and then incubated in buffer containing the Vector avidin-biotin-HRP complex (~50 μl of kit solution A, ~50 μl of kit solution B in 2.5 mls of 0.1 M phosphate buffer) for 3 h. The tissue was then rinsed in buffer for 1 h and standard HRP histochemistry was performed using diaminobenzidine (DAB) as the substrate for the HRP reaction. The retinas were mounted on a slide vitreal side up, dehydrated, cleared, and coverslipped without counterstaining.

Soma diameter was determined by entering an outline of the soma, traced at 1500× with a drawing tube, into a computer *via* a graphics tablet. Soma diameter was expressed as the diameter of a circle with the same area. To calculate dendritic field area, a convex polygon was traced around the dendritic field perimeter at 400× and entered into the computer. Dendritic-field diameter was expressed as the diameter of a circle with the same area as that of the polygon.

Results

Parasol but not midget cells show tracer coupling

The pattern of intracellular staining after Neurobiotin injection into midget and parasol cells was distinctive and reproducible (Fig. 1). Both midget ($n = 70$) and parasol cells ($n = 186$) showed a Golgi-like staining of the dendritic tree (Fig. 2A) that was similar in appearance to the results of intracellular injections of HRP (Watanabe & Rodieck, 1989). Midget cells showed no evidence of tracer coupling either in the fovea (Fig. 1E) or extrafoveal retina (Fig. 1D). By contrast the majority of injected parasol cells ($n = 121$; 65%) showed a characteristic pattern of cellular labeling of neighboring parasol cells (homotypic coupling) and amacrine cells (heterotypic coupling) (Figs. 1 and 2). Some of the amacrine cells showed relatively intense staining of somata and dendritic tree while in others the dendrites were very lightly stained or unstained. In many instances, an amacrine cell's morphology was revealed in sufficient detail that at least two tracer-coupled amacrine cell types could be distinguished, as will be shown below.

Homotypic coupling between parasol cells of the same type

For each of the Neurobiotin-filled parasol cells that showed coupling, three to six nearby somata were also lightly stained; they were the same size as the injected cell and were located in the ganglion cell layer (Figs. 1,2, and 4). These tracer-coupled

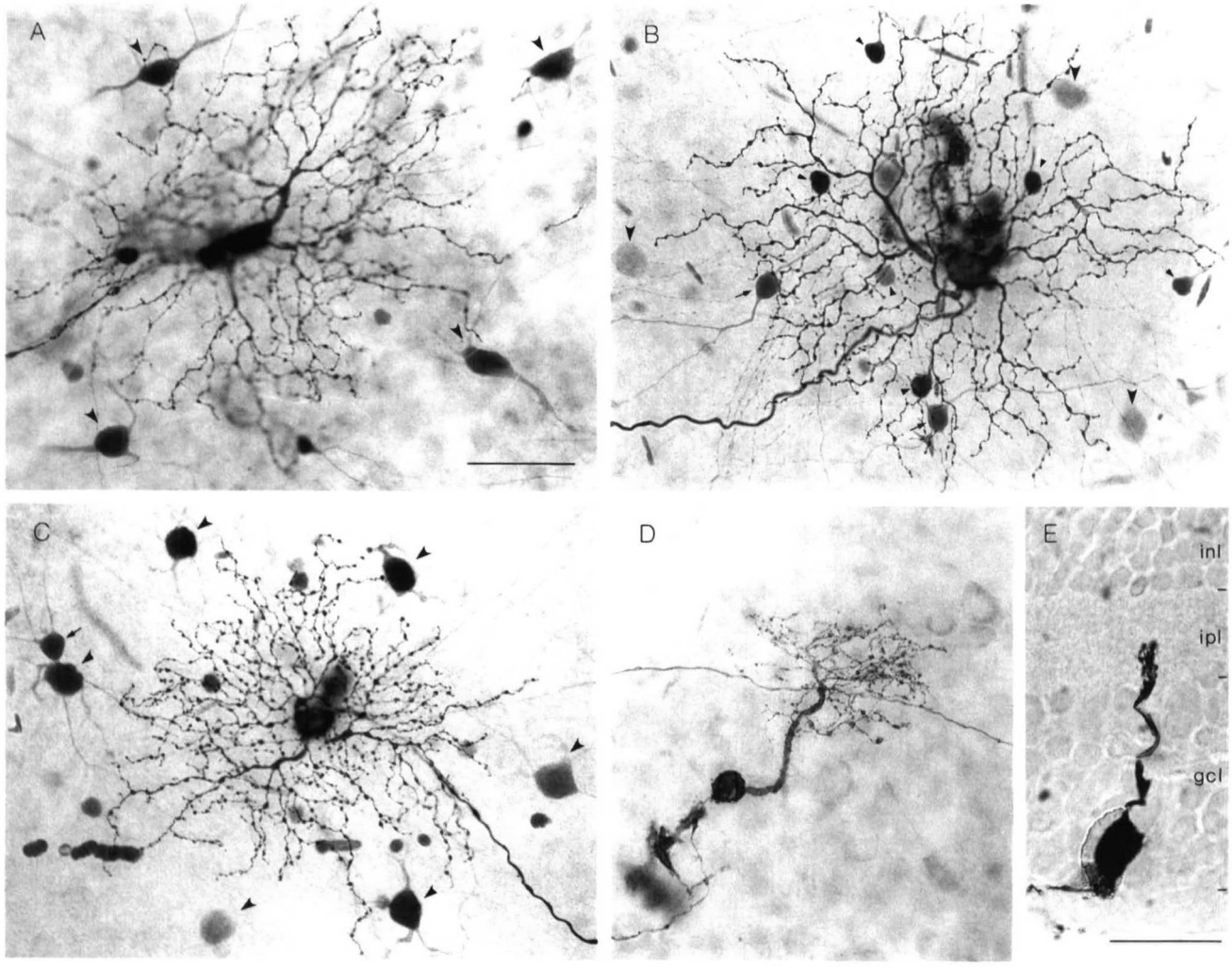

Fig. 1. Photomicrographs of intracellular Neurobiotin-fills of parasol and midget ganglion cells in wholemounts of *M. nemestrina* retina. A: The arrowheads indicate somata of neighboring parasol cells tracer coupled to injected cell. B: Parasol cell, peripheral retina. Tracer-coupled parasol cells are only lightly stained (large arrowheads); large and small tracer-coupled amacrines are intensely stained and are indicated, respectively, by the small arrows and small arrowheads. C: Parasol cell, peripheral retina. Tracer-coupled parasol cell neighbors are intensely stained (arrowheads); one large amacrine is indicated by the small arrow. D: Midget cell, peripheral retina. E: Vertical section through foveal midget cell; retinal eccentricity: 600 μm. No tracer coupling was observed for any Neurobiotin-filled midget cells ($n = 70$). Scale bar = 50 μm for A-D; 25 μm for E. inl: inner nuclear layer; ipl: inner plexiform layer; and gcl: ganglion cell layer.

cells were typically arrayed around the periphery of the parasol dendritic tree with a regular spacing suggestive of a mosaic of cells of the same type (Wässle et al., 1981). In some cases, the proximal dendrites of the coupled cells appeared to costratify with the injected cell. Taken together, the soma size, dendritic stratification, and regular spacing of the large tracer-coupled cells indicated that all were parasol cells of the same type, either inner branching (presumed ON-center) or outer branching (presumed OFF-center). A consistent feature of this homotypic coupling was that, regardless of the intensity of staining of the injected and tracer-coupled cells, only the apparent nearest neighbors showed tracer coupling (Fig. 2C). The significance of this pattern for understanding the basis for the coupling will be taken up in the Discussion.

There were no obvious morphological differences between injected parasol cells that showed tracer coupling and those that did not. A scatter plot of dendritic-field diameter *vs.* retinal eccentricity for both the coupled and noncoupled cells showed that both groups formed a single cluster along this dimension (Fig. 3). Because only 65% of the parasol cells showed tracer coupling, we considered the possibility that only the ON-center or only the OFF-center parasol cell types were coupled. To determine if this was the case, we made intracellular fills of several closely spaced pairs of parasol cells. By focusing through their overlapping dendritic trees in the retinal wholemount, it was possible to distinguish the relative difference in stratification between inner (ON-center) and outer (OFF-center) branching types. For four such overlapping cell pairs, homotypic coupling occurred for both the inner and outer branching parasol cells. Thus when the dendritic trees of an injected inner/outer cell pair were almost completely overlapping, the number of coupled cells that surrounded the two trees was typically about twice that observed after a single parasol cell was injected.

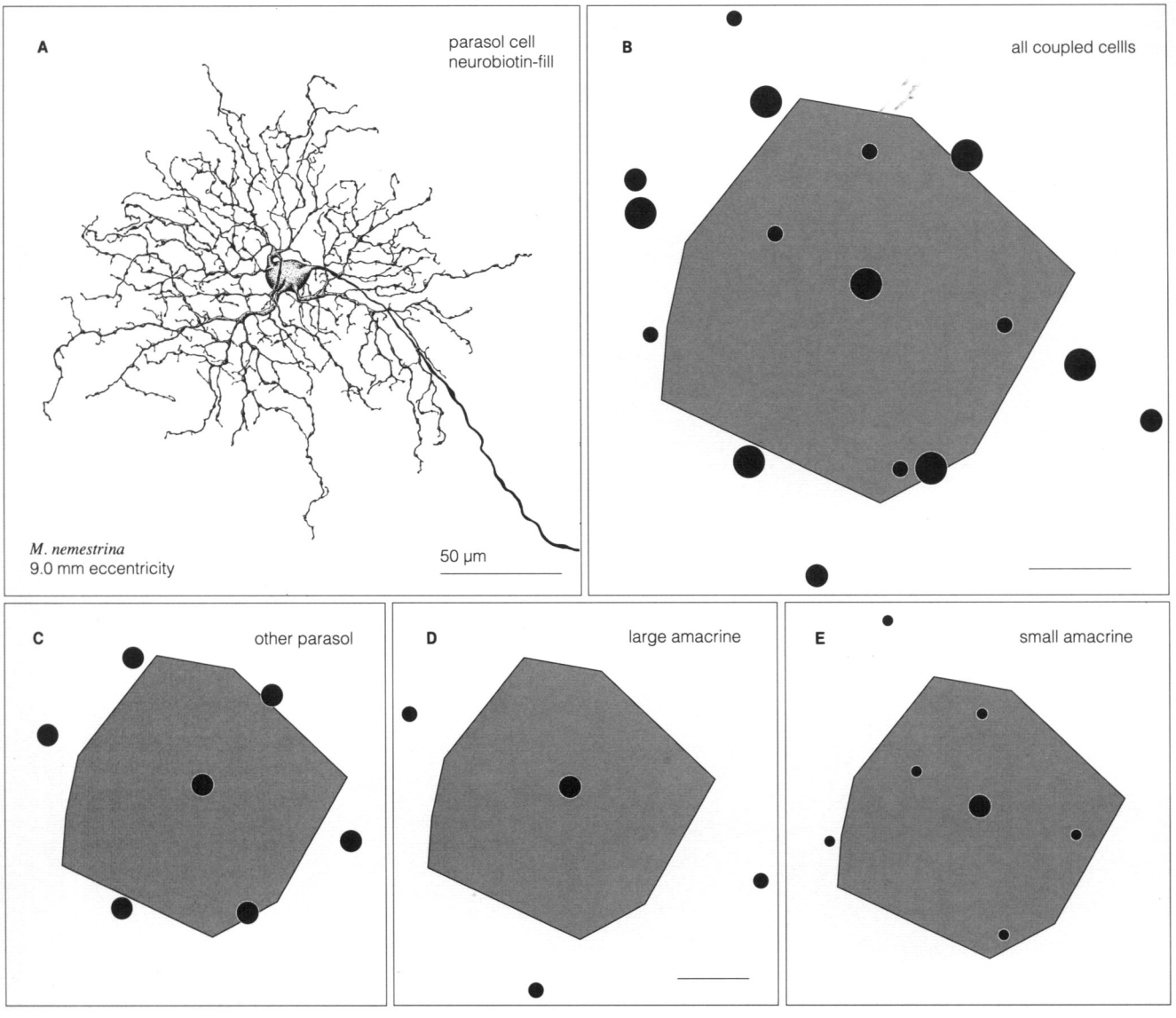

Fig. 2. Camera lucida tracing of a Neurobiotin-filled parasol cell and pattern of associated tracer-coupled cells. A: Morphology of the parasol cell dendritic tree. Stratification of dendritic tree indicated that this cell was an inner branching (presumed ON-center) type. B: Dendritic tree of the injected cell is indicated by the shaded polygon. The somata of other cells that also showed Neurobiotin staining are illustrated by the filled circles. Large circles indicate parasol cell bodies, medium circles indicate large amacrine cell bodies, and small circles indicate small amacrine cell bodies. C: Pattern of coupling to neighboring parasol cells. Note the regular spacing of the neighboring parasol cells around the periphery of the injected cell's dendritic tree. D: Pattern of coupling to large amacrine cells with intensely stained dendrites. E: Pattern of coupling to small amacrine cells with faintly stained dendrites. The small amacrines were consistently more closely spaced and numerous than the large amacrines. All scale bars = 50 μm.

Homotypic coupling reveals constant dendritic overlap from central to peripheral retina

The tracer coupling of neighboring parasol cells made it possible to determine the relationship of dendritic overlap to retinal eccentricity for this cell type. Previously, it has been shown for other ganglion cell types that an inverse relationship between dendritic-field size and cell density results in a constant dendritic-field overlap from central to peripheral retina (for review see Wässle & Boycott, 1991). Thus, as dendritic-field sizes increase, the distances between neighboring cells of the same type increase as a constant fraction of the dendritic-field size. This same pattern was apparent in the tracer-coupled parasol cell clusters over a range of eccentricities (Fig. 4A). Tracer-coupled cells were always located around the perimeter of the injected cell's dendritic tree. This distance, which is slightly greater than half of the dendritic-field diameter, was maintained as the dendritic tree increased in size fourfold from 3–15 mm retinal eccentricity. This relationship was quantified by measuring the distance from each labeled parasol cell in a coupled cluster to its nearest neighbor. The mean of the nearest-neighbor values for each cluster was plotted against dendritic-field diameter (Fig. 4B). The best-fitting straight line to the data showed that the nearest-neighbor distance remains a constant fraction of

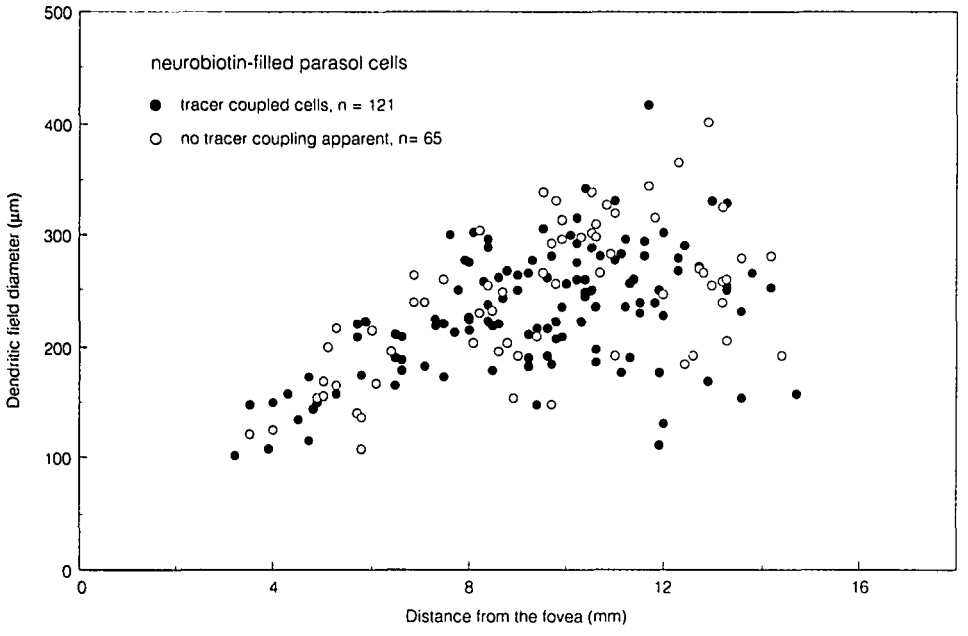

Fig. 3. Scatterplot of dendritic-field diameter *vs.* retinal eccentricity for the Neurobiotin-filled parasol cells. 186 parasol cells, ranging in eccentricity from 3–15 mm, were injected with Neurobiotin. 65% of the injected cells showed homotypic and heterotypic tracer coupling (filled symbols) as illustrated in Fig. 1. The cells that did not show tracer coupling (open symbols) occupied the same dendritic-field size and eccentricity range as the coupled cells.

dendritic-field size (ratio of diameter to nearest-neighbor distance = 1:0.62). The parasol cells therefore maintain a constant dendritic-field overlap over a wide range of retinal eccentricities.

Heterotypic coupling in parasol cells occurs with at least two distinct amacrine cell types

Differences in soma size, dendritic morphology, intensity of staining, and cell density suggested that two distinct amacrine cell types were tracer coupled to the parasol cells (Figs. 5A and 5B). One type had a relatively large soma and a dendritic tree that often stained intensely and completely (cell bodies indicated by large arrowheads in Figs. 5A and 5B). The other type had a smaller soma and usually very lightly stained or unstained dendrites, although in several instances the entire dendritic tree was revealed (cells indicated by small arrowheads in Figs. 5A and 5B).

When the stained amacrine cells were sorted into a group that showed little or no dendritic staining and a group that showed intense dendritic staining, two distinct soma size distributions were found (Fig. 6). Mean soma diameter for cells with lightly stained or unstained dendrites (8.4 ± 1.8 μm) was smaller than the mean for cells that showed intense dendritic staining (10.7 ± 2.0 μm). For both the large and the small amacrines the laminar location of the cell body was variable. Tracer-coupled amacrine somata were found in the inner nuclear layer, the inner plexiform layer, and the ganglion cell layer. For the majority of cells, the soma appeared to be in either the inner plexiform layer or the ganglion cell layer. Thus, the laminar position of the cell body did not appear to be a useful criterion for grouping the cells and no attempt was made to quantify this variable.

The dendritic morphology of these two groups of amacrine cells was quite distinct (Fig. 7). The larger amacrine cell had relatively thick, smooth proximal dendrites that branched sparsely. The dendrites extended for about 200–300 μm from the soma and then tapered abruptly into extremely thin processes that were studded with varicosities (Fig. 7, arrowheads). These thin processes also occasionally arose as side branches from along the thick main dendrites. Each of the thin, axon-like processes could be traced in the inner plexiform layer for 2–3 mm before the HRP reaction product faded (Fig. 7, lower inset). These axon-like processes occasionally passed through the dendritic field of a Neurobiotin-filled parasol cell and appeared to be narrowly stratified at the same level as the parasol cell dendrites. Thus, both the thick dendritic processes and the thin, axon-like components of the large amacrine cell type appear to costratify with the parasol cell dendrites.

The smaller amacrine cell type also had a very large, sparsely branching dendritic tree, but the dendrites were extremely thin compared to the proximal dendrites of the larger amacrine cell type (Fig. 7). These dendrites did not show any evidence of a division into dendritic and axon-like components that was apparent for the larger cell type. In a few instances, the dendritic tree of the smaller amacrine could be traced completely and showed unbranched processes that extended for ~1–2 mm before terminating abruptly (Fig. 7, upper inset). These cells therefore had dendritic-field sizes that were smaller than the overall extent of the larger amacrine.

Another difference between the two groups of amacrine cells was that the spatial density of the smaller cells was higher than that of the larger cells. This pattern is illustrated in Figs. 2 and 8. The large amacrines typically showed a near-neighbor spacing of ~250 μm. By contrast the small amacrines showed a spacing of about 100–150 μm. Because the staining pattern of the amacrine cells was somewhat patchy and irregular, no attempt was made to quantify their spacing more precisely. It thus appears likely that these two groups of cells represent distinct amacrine cell subpopulations that each show a characteristic morphology, cell density, and mosaic organization.

Possible site of cellular coupling between the parasol and amacrine cells.

A likely site for the cellular coupling between the large amacrines and the parasol cells was a close apposition between the

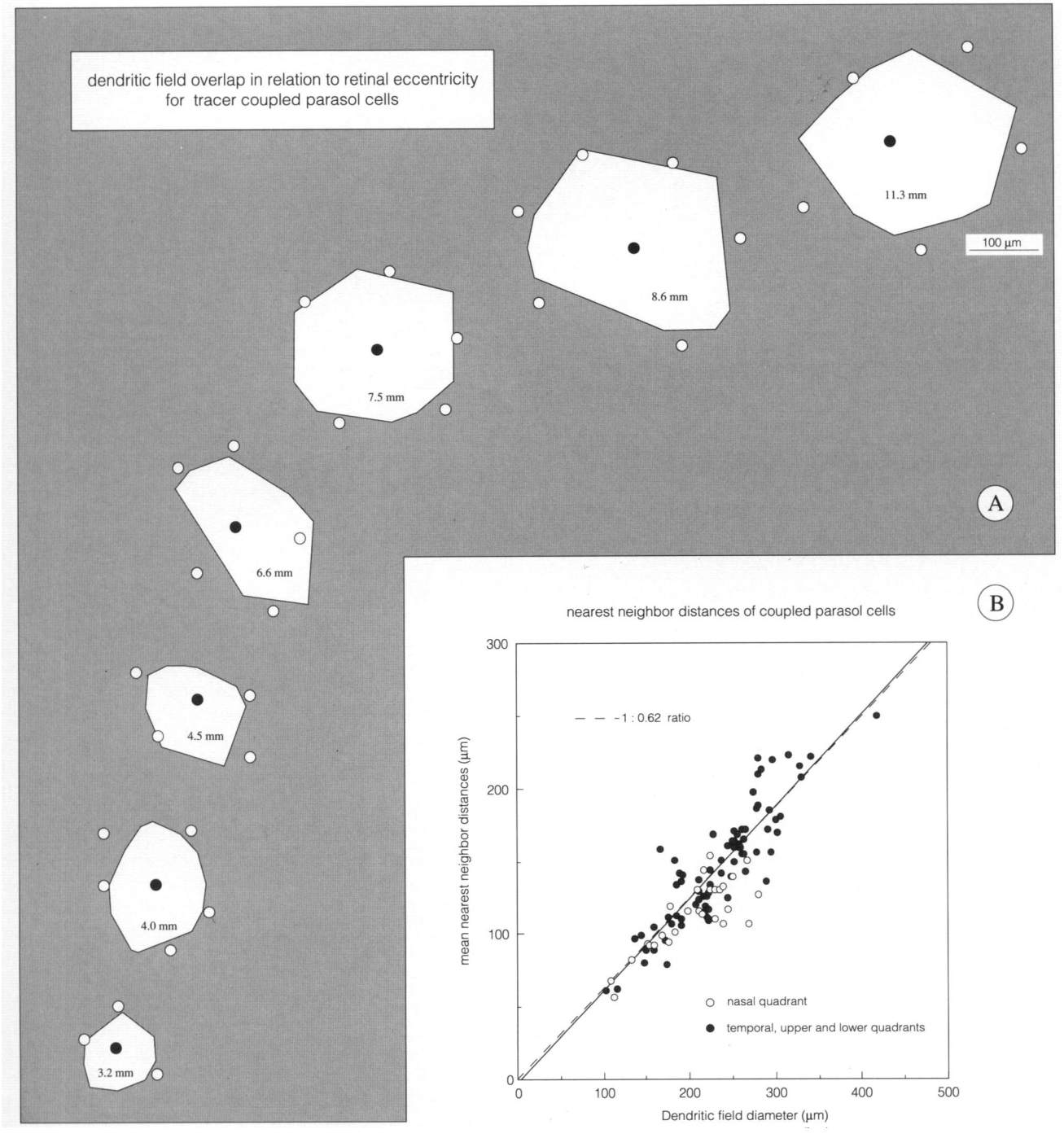

Fig. 4. Homotypic coupling for parasol cells at a range of retinal eccentricities. A: The polygons were traced around the extremities of the dendritic tree for each parasol cell and the retinal eccentricity of the injected cell body (filled circle) is indicated within each polygon. The cell bodies of the tracer-coupled cells are indicated by the open circles surrounding each polygon. At each eccentricity the coupled cells are located around the periphery of the dendritic field suggesting that the degree of dendritic-field overlap remains constant at different eccentricities. B: Scatterplot of dendritic-field diameter for each Neurobiotin-filled parasol cell *vs.* the mean of the nearest-neighbor distances for each cell in a coupled cluster. The solid line was fit by linear regression through the data points from the temporal upper and lower quadrants ($R = 0.89$; $y = -1.92 + 0.633x$). The dashed line marks a diameter to nearest-neighbor distance ratio of 1:0.62 and closely matches the regression line.

parasol cell dendrites and the proximal, thick dendrites of the large amacrine cell. Short lengths of the amacrine dendrite (~20–100 µm) often apposed the injected parasol dendrite and followed its wavy course (Figs. 5C and 5D). By contrast, the axon-like components of the large amacrine cell appeared to be unlikely candidates for the site of coupling since these processes typically arose from the distal tips of the main dendrites beyond the margin of the injected parasol dendritic tree. In the few instances, where an axon-like process was present within the parasol dendritic field, no appositions with a parasol dendrite were observed.

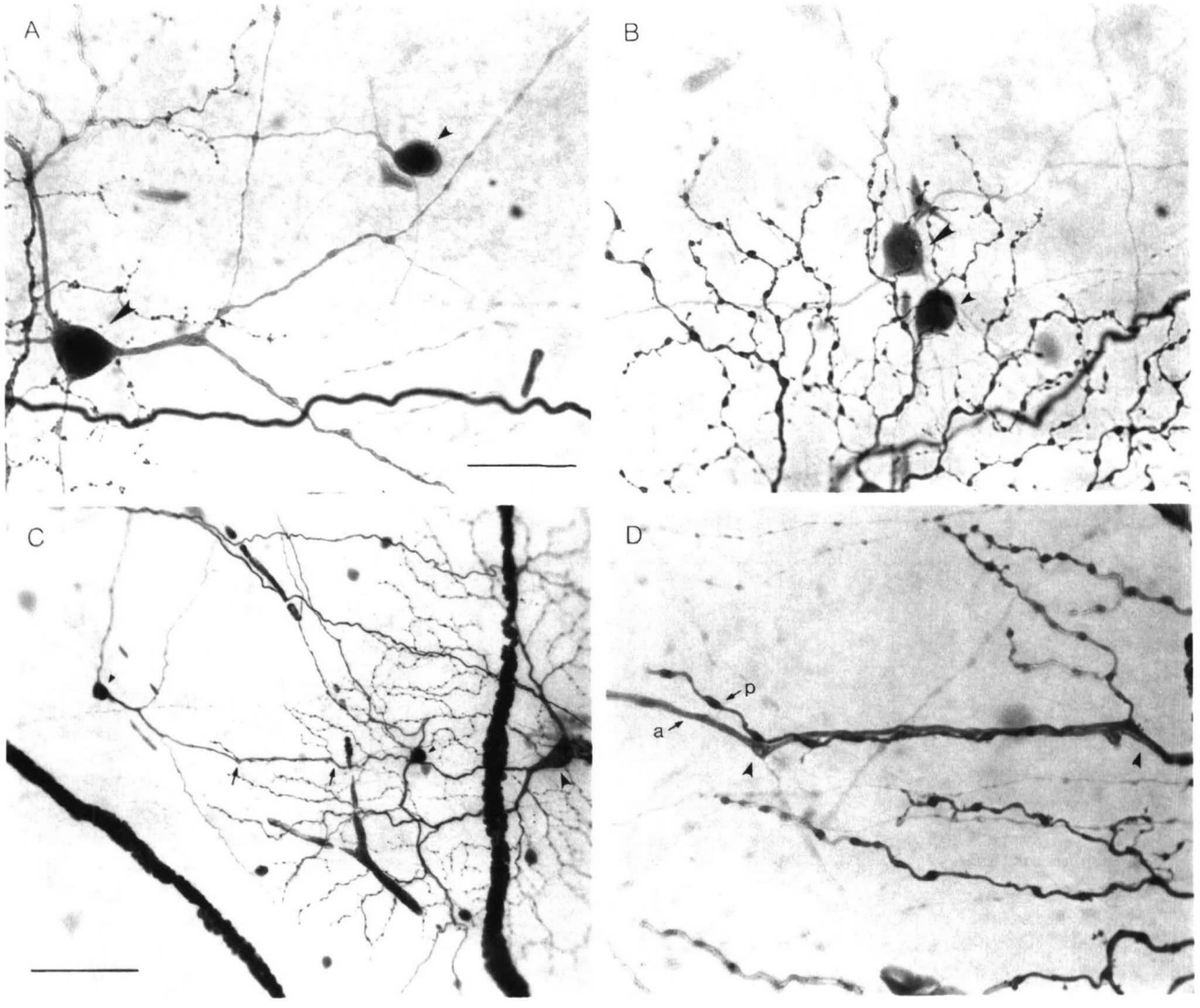

Fig. 5. Photomicrographs of amacrine cells tracer coupled to Neurobiotin-filled parasol cells. A,B: Two examples of large and small amacrine cells (indicated respectively by the large and small arrowheads) at the periphery of a parasol cell dendritic tree. C: Two large amacrines (cell bodies indicated by small arrowheads) coupled to an injected parasol cell (large arrowhead). A close apposition of an amacrine dendrite with a parasol cell dendrite is indicated by the two arrows. This apposition is shown at higher magnification in D. D: The amacrine cell dendrite (indicated by the arrow and labeled *a*) is more lightly stained and follows the course of the more darkly stained parasol dendrite (indicated by the arrow and labeled *p*).

Discussion

Comparison with cat ganglion cells

The detailed pattern of both homotypic and heterotypic tracer coupling revealed by intracellular Neurobiotin injection of macaque parasol cells appeared strikingly similar to that observed for alpha cells of the cat's retina (Vaney, 1991). For both parasol and alpha cells, homotypic coupling occurred between the injected cell and several surrounding cells. These cells appeared to be the nearest neighbors of the same type and were stained with light to moderate intensity. The pattern of amacrine cell coupling after parasol cell injection also paralleled that observed for alpha cells. Details of the amacrine cell coupling to alpha cells have not yet been reported, but it was noted that more than a single amacrine cell type appeared to be stained and that the laminar location of the cell bodies included the inner nuclear layer, inner plexiform layer, and ganglion cell layer (Vaney, 1991). In addition, it was suggested that one of the amacrine types might correspond to the "long-range" amacrine cells described in silver-stained cat and rabbit retina (Vaney et al., 1988). In the cat this amacrine cell type shows the abruptly tapered dendrites and the long, axon-like processes that were observed for the large amacrine cells coupled to parasol cells (Fig. 7). Both alpha and parasol cells thus seem to be coupled to an equivalent amacrine cell type that gives rise to multiple, axon-like processes.

This correspondence in tracer coupling supports the proposition that the parasol cells are the primate equivalent of the cat alpha cells (Leventhal et al., 1981; Rodieck et al., 1985), and argues against the suggestion that parasol cells are equivalent to cat beta cells and that no alpha cell homologue has been identified in the primate retina (Shapley & Perry, 1986; Silveira & Perry, 1991). Similarly, the apparent lack of coupling for both

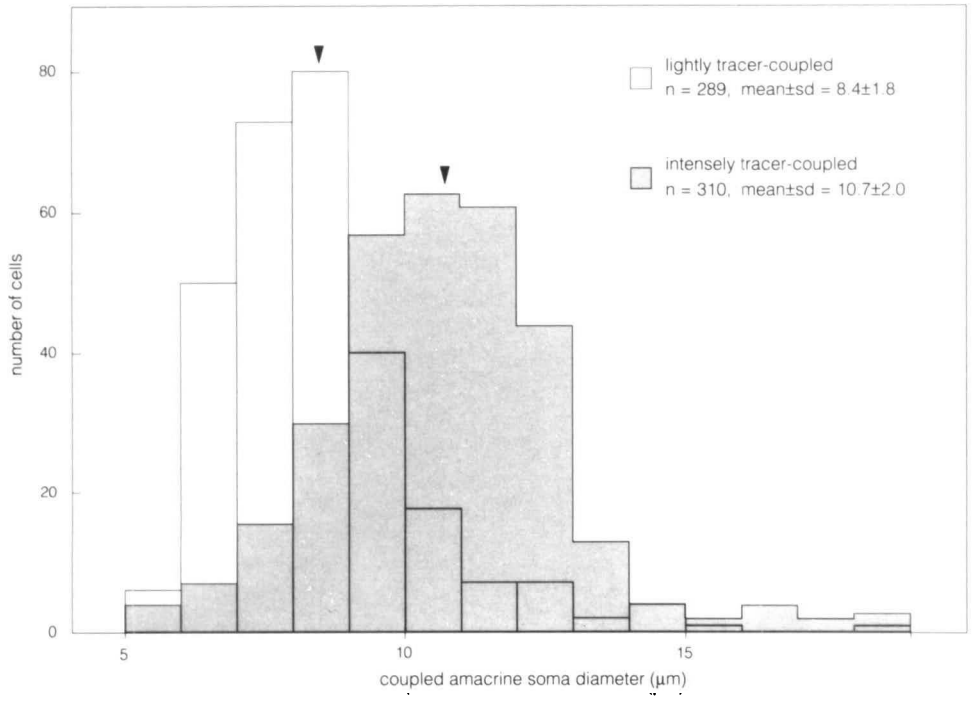

Fig. 6. Soma size analysis of tracer-coupled amacrine cells suggests that two distinct amacrine cell subpopulations were stained. The stained amacrine cells fell into two distinct groups on the basis of staining intensity. One group of cells showed intense staining of both cell body and much of the dendritic tree (n = 310). The other group showed only lightly stained or unstained dendrites (n = 289). The histogram shows a distinct soma size distribution for each group. The mean soma size for each group is indicated by the arrowheads above the histogram.

the beta cells and midget cells is further evidence for their equivalence.

Types of amacrine cells coupled to parasol cells

The morphologies of the large and small tracer-coupled amacrine cells were revealed in enough detail to allow comparison with previous studies of mammalian amacrine cell types. As discussed above, the axon-like component of the large amacrine suggested a correspondence with the "long-range" neurofibrillar-stained amacrine cells that have been found in the cat and rabbit retina (Vaney et al., 1988). In primate retina, amacrine cells with a similar morphology have been observed in Golgi preparations (Rodieck, 1988; Mariani, 1990). However, several other amacrine cell types have been recently described in the macaque and cat retina that show both axon-like and dendritic processes. It is possible that any one of these identified cell types might correspond to the large tracer-coupled amacrine.

One identified amacrine cell type is a tyrosine-hydroxylase-immunoreactive cell that has been shown in both cat and macaque to give rise to long, axon-like processes (Dacey, 1990*a*, *b*). However, this cell type is unlikely to be the large tracer-coupled amacrine because the axon-like processes arise close to the cell body and both the dendrites and the axon-like processes stratify principally at the outer border of the inner plexiform layer. A second "axon-bearing" amacrine cell type of the macaque retina (Dacey, 1989*a*) can also be easily distinguished from the large tracer-coupled amacrine by many aspects of its distinctive morphology. For example, both the dendritic and axonal arbors are highly branched when compared with the large tracer-coupled amacrine. In the cat's retina, a monoamine-accumulating amacrine cell type has been observed that also shows long axon-like processes, and is similar to the large tracer-coupled amacrine in that the axon-like processes arise by an abrupt taper of each of the main dendrites (Dacey, 1988). However, it too can be distinguished from the large tracer-coupled amacrine by dendrites that are spiny and bear many short branchlets. Finally, somatostatin-immunoreactive amacrine cells show long projecting, axon-like processes but they can be easily distinguished from the large tracer-coupled amacrines by their restricted location in the ventral retina and the unique asymmetrical projection of the "axon" into the dorsal retina (Sagar, 1987; Sagar & Marshall, 1988; White et al., 1990). In summary, several amacrine cell types that clearly show a dual dendritic and axon-like morphology have been previously identified; all of these types, with the possible exception of a neurofibrillar-stained cell observed in cat and rabbit, can be clearly distinguished from the large tracer-coupled amacrine by differences in stratification and/or the morphology of the axon-like and dendritic components.

The morphology of the small tracer-coupled amacrine cell appears to most closely resemble a type of serotonin-accumulating and GABA-immunoreactive amacrine cell type observed recently in the cat's retina (Wässle & Chun, 1988; Wässle et al., 1987). In primate retina, amacrine cells with a similar morphology have been observed in Golgi preparations (Mariani, 1990). These cells, like the small tracer-coupled amacrines, have small somata, ~8–9 μm in diameter and a sparsely branching dendritic tree. The dendrites are extremely thin and extend for about 2 mm without branching or showing any distinct morphological specializations (see Wässle et al., 1987; their Fig. 4A). Analysis of retinal wholemounts suggested that this cell type stratifies in the middle third of the inner plexiform layer (between 40–80% depth). The inner and outer branching types of macaque parasol cells and cat alpha cells stratify at about the 40% and 70% level of the inner plexiform layer and it is therefore possible that this amacrine cell type costratifies with the parasol and alpha cell.

Is the homotypic coupling mediated by the large amacrine cells?

As noted by Vaney (1991), the presence of both homotypic and heterotypic coupling leaves open the possibility that the homo-

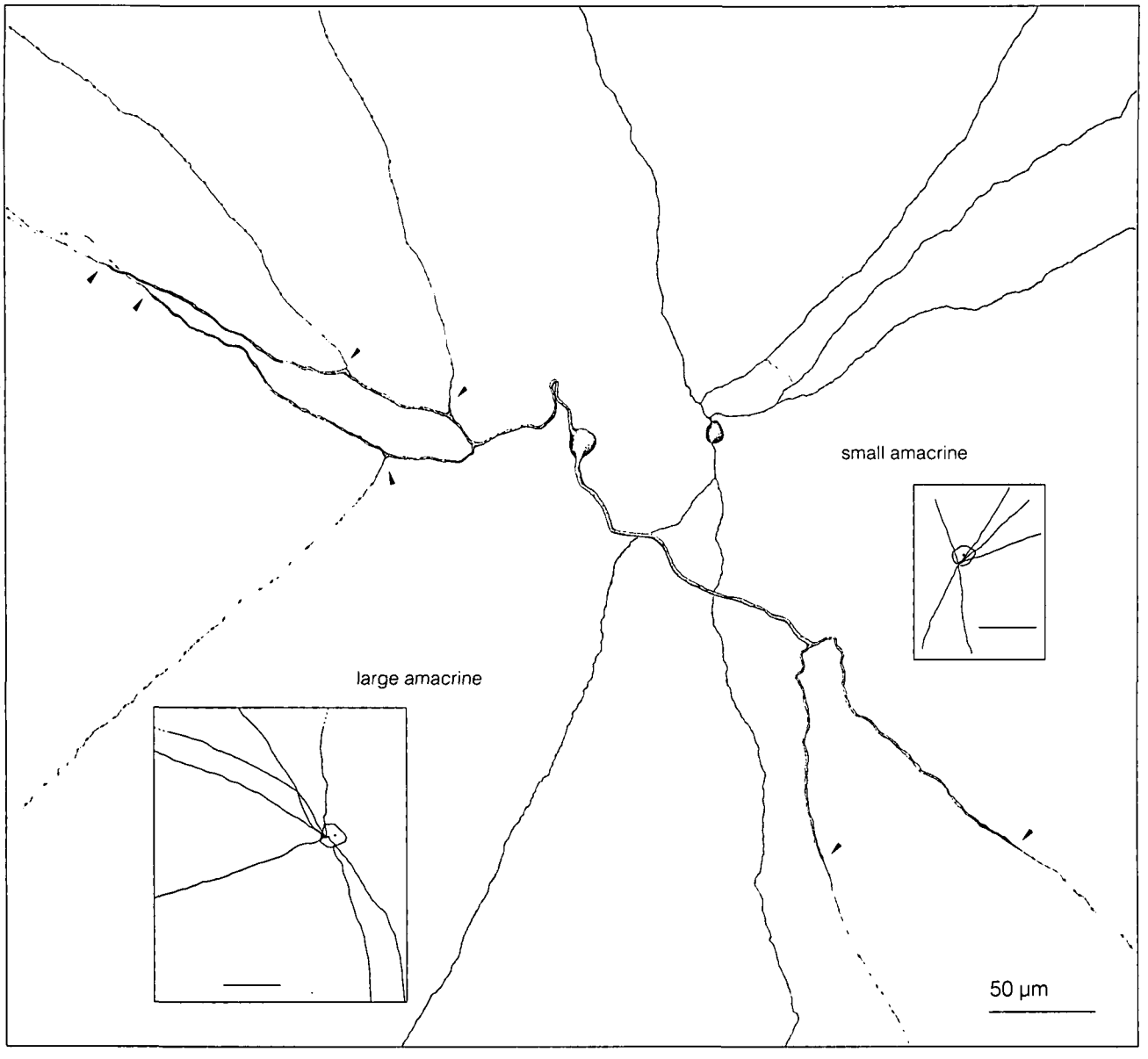

Fig. 7. Morphology of amacrine cells coupled to parasol cells. This figure shows examples of the dendritic branching pattern of the large and small tracer-coupled amacrine cell types. The larger cell has long axon-like processes that have been traced for over 2 mm from the cell body. Arrowheads indicate points on the main dendrites where they abruptly tapered to thin, axon-like processes. Inset on the left shows a tracing of an entire cell and its relation to the intracellularly injected parasol cell dendritic tree (polygon). The smaller cells also have large, sparsely branched trees but compared to the large amacrine cells the dendrites are thin and show no evidence for distinct axon-like processes. Inset on the right shows the complete tracing of this cell. Scale bar in both insets = 1 mm.

typic tracer coupling may take place indirectly *via* the amacrine cells. There is no way at present to distinguish unequivocally between direct or indirect coupling but at least three features of the overall coupling pattern suggest that the homotypic coupling may be indirectly mediated by the dendrites of the large and/or small amacrine cell types (Fig. 9). First, a consistent feature of the parasol-parasol coupling is that only the nearest neighbors of the injected cell show tracer coupling (Fig. 9A). If the parasol cells were coupled directly to each other, it might be expected that the tracer coupling would, at least in some instances, extend beyond the neighboring cells and progressively decrease in intensity with distance from the injected cell. Such a pattern has been observed after intracellular Neurobiotin injections into AII amacrine cells (Vaney, 1991; Dacey, unpublished observations), where the presence of gap junctions between cells of the same type has been well established (Famiglietti & Kolb, 1975; Dacheux & Raviola, 1986), and for a bistratified ganglion cell type in the rabbit retina that showed homotypic tracer coupling only (Vaney, 1991). Second, the only site of potential coupling observed in the present results was the close apposition of the main dendrites of the large amacrine cells with the dendrites of the injected parasol cell (Figs. 5C, 5D, and 9B). Third, the diameter of the proximal dendritic tree of the large amacrine (where the close appositions take place) closely matches the size of the region over which the homotypic coupling takes place. This suggests that the Neurobiotin is transferred from the in-

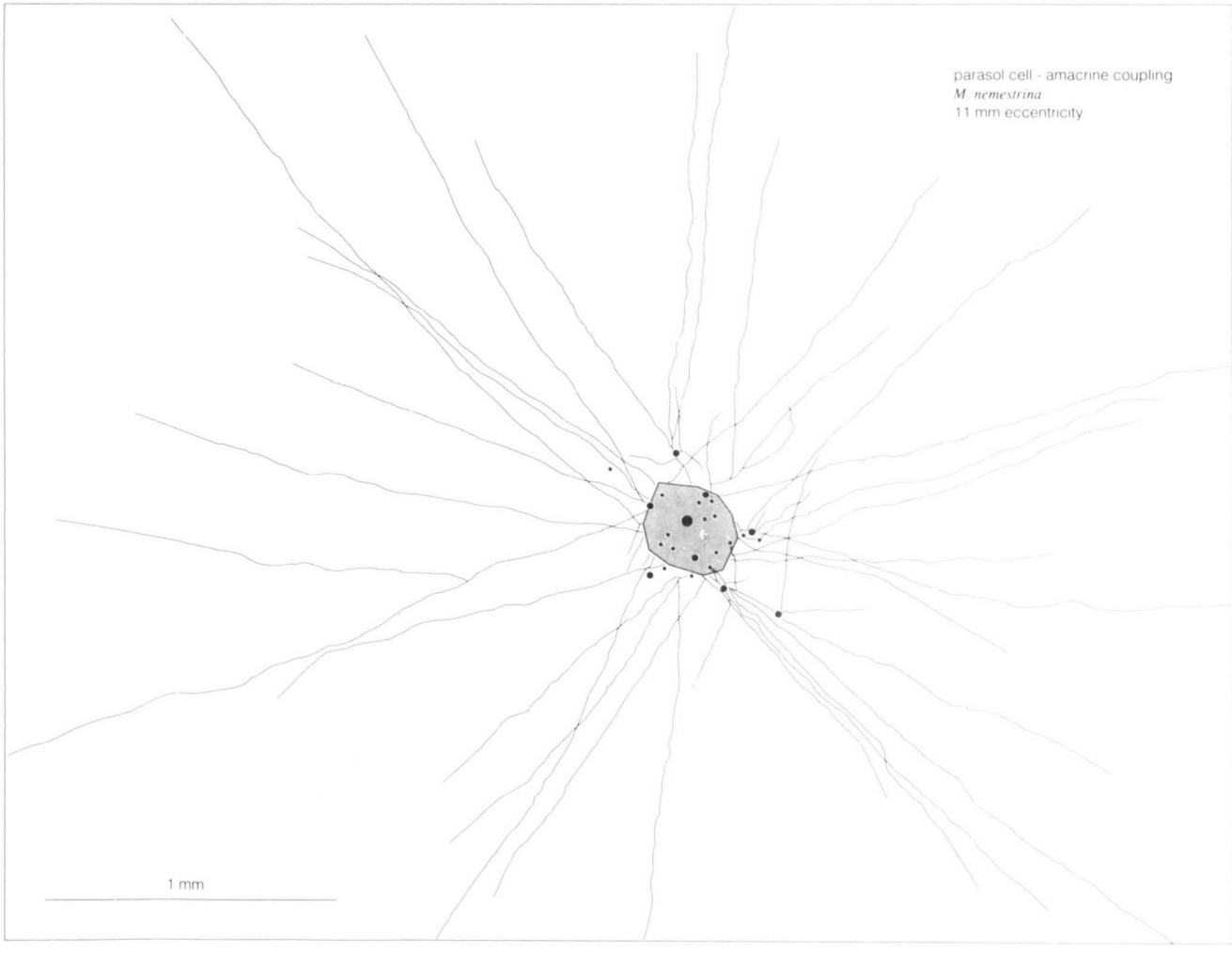

Fig. 8. Network of long axon-like processes that are stained after intracellular Neurobiotin-fill of a single parasol ganglion cell. In this tracing, the parasol dendritic tree is outlined by the polygon in the center. The cell bodies of all the tracer-coupled amacrine cells are illustrated by the small filled circles in the vicinity of the dendritic tree. The small and large filled circles correspond, respectively, to the small and large amacrine cells. The long, axon-like processes of the amacrine cells extend radially away from the region of the parasol dendritic tree for ~2–3 mm before they either terminate or could not be traced further because the HRP reaction product gradually diminished.

jected parasol cell to neighboring parasol cells by the dendrites of the large amacrine cells (Figs. 9C and 9D). This explanation would account for the restricted pattern of labeling of both the parasol and large amacrine cell: the large amacrine and parasol cells are coupled to each other but neither cell type is coupled directly to itself. This indirect coupling hypothesis does not incorporate the long axon-like processes of the large amacrine cell which are not suitably positioned for playing a role in the heterotypic coupling. These processes would presumably play a very different functional role in the interactions between the large amacrine cells and the parasol cells.

The hypothesis of indirect coupling is consistent with the finding that neighboring alpha cells can excite each other (Mastronarde, 1983). Mastronarde argued persuasively that gap junctions between neighboring alpha cells of the same center sign were the most likely explanation for his findings, and the observation of tracer coupling between neighboring alpha cells appears to support Mastronarde's hypothesis. However, Mastronarde also pointed out that the presence of an intermediate neuron was equally plausible if this interneuron had very selective connections with the alpha cell (so as to prevent current spread to other ganglion cell types). The present results strongly point to the existence of quite selective connections between the parasol ganglion cell and an amacrine cell type.

Does coupling contribute to the center size of the parasol receptive field?

The present results, and those of Vaney (1991), suggest that gap junctional coupling of parasol and alpha cells with large field amacrine cells in the inner plexiform layer could mediate the spread of local excitation beyond a single dendritic tree. In the macaque retina, measurements of receptive-field center size for the phasic, nonopponent ganglion cells (presumed parasol cells) suggested that dendritic-field size was about the same as the receptive-field size (De Monasterio & Gouras, 1975; Crook et al., 1988), but it has not been technically possible to directly compare the receptive-field size for a recorded parasol cell with the size of its dendritic tree. However, in cat retina it has been shown that at mesopic luminance levels the receptive-field cen-

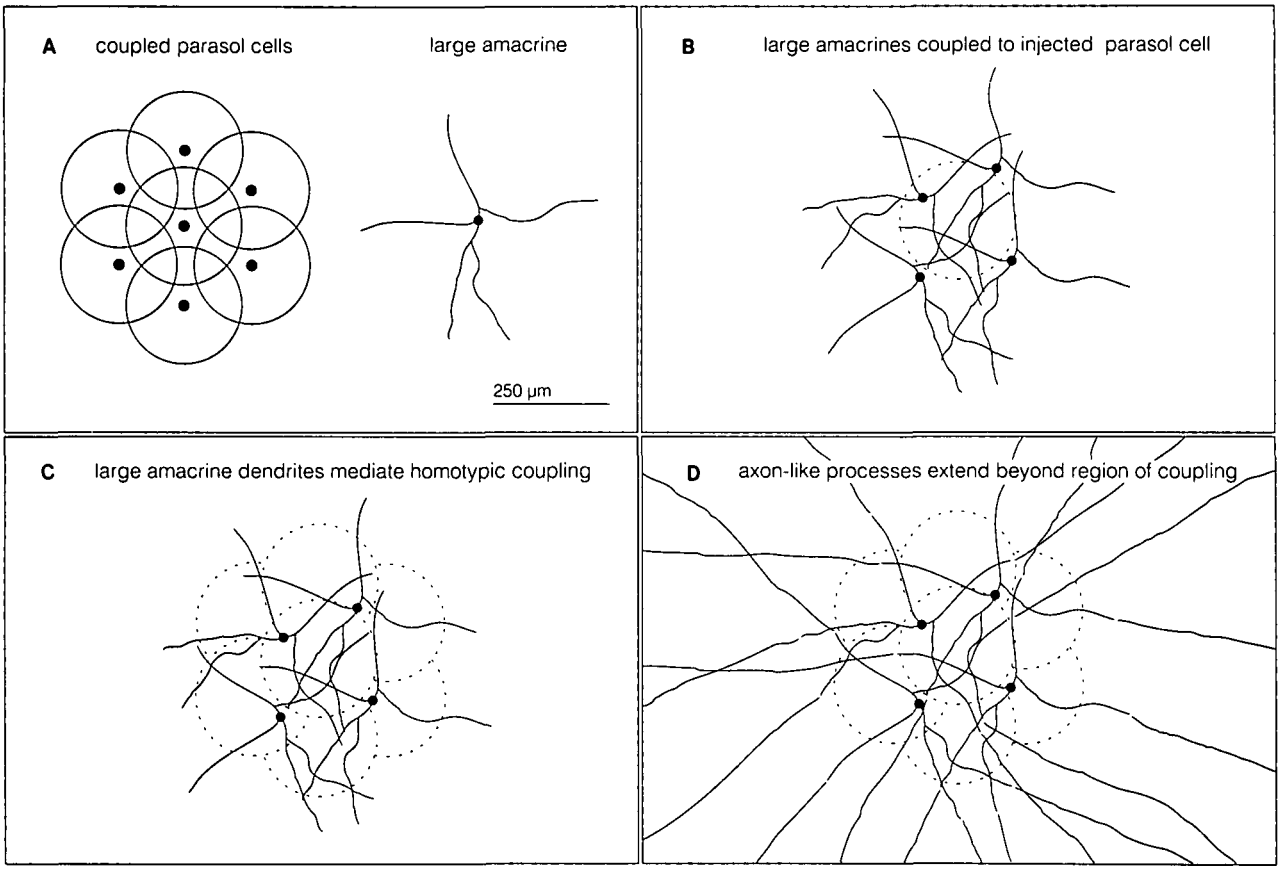

Fig. 9. Hypothesis for the basis of homotypic and heterotypic tracer coupling. A: The parasol-parasol coupling is restricted to the nearest neighbors of the injected cells. The overlapping dendritic fields are illustrated by the circles with cell bodies placed in a hexagonal array. The main dendrites of the large amacrine cell are the apparent site of heterotypic coupling with the parasol cells; these dendrites form a field with a diameter that is about the same as that of the cluster of coupled parasol cells. B: Only the large amacrine cells whose dendrites make contact with the injected parasol cell show tracer-coupling. C: The dendrites of the tracer-coupled amacrines that extend beyond the dendritic field of the injected parasol cell make junctional contact with the adjacent parasol cells and provide the pathway by which the Neurobiotin reaches only the nearest-neighbor parasol cells. D: The axon-like processes extend beyond the dendritic trees of the cluster of parasol cells and are not involved in either the homotypic or heterotypic tracer coupling.

ters for alpha ganglion cells are at least twice as large in area as the dendritic tree (Peichl & Wässle, 1983). One explanation offered for the increase in receptive-field over dendritic-field size is that synaptic contacts with cone bipolar and small field amacrine cells at the peripheral edge of the dendritic tree could enlarge the receptive-field center size beyond the dendritic tree size (Peichl & Wässle, 1983). A problem with this suggestion is that it would only account for a very small increase in receptive-field over dendritic-field size. On the other hand, the presence of homotypic coupling points to a mechanism that could significantly increase receptive-field size over dendritic-field size for the parasol and alpha ganglion cells.

Functional significance of a coupled network for parasol cells but not midget cells

The coupling of a distinct amacrine cell network to parasol cells, but apparently not to midget cells, predicts significant differences in the synaptic connections with amacrine cells for the two ganglion cell classes which should have a physiological correlate. One striking difference between the light-driven response of the midget and parasol cell is that the contrast sensitivity of the parasol cell is about 8–10 times greater than that for midget cells at both scotopic and photopic levels of illumination (Kaplan & Shapley, 1986; Purpura et al., 1988). This difference enables the parasol cell but not the midget cell to respond well to spatial patterns at low light levels. The neural basis for this large difference in sensitivity is not known but one suggestion is that it is a result of the parasol cell's larger receptive-field size. This argument is based on the idea that the overall sensitivity of the cell's receptive field at a given light level is proportional to the area of the receptive-field center. The results of the present study suggest that gap junctions with wide-field amacrine cells could be a mechanism, absent in the midget cell population, that serves to increase receptive-field size and response sensitivity of parasol cells.

Acknowledgments

This work was supported by NIH Grant EY06678 (to D.M.D.) and by NIH Grant RR00166 to the Regional Primate center at the University of Washington. We thank Christine Curcio, David Marshak, Kate Mulligan, Helen Sherk, and two anonymous reviewers for their helpful comments on the manuscript.

References

BOYCOTT, B.B. & WÄSSLE, H. (1991). Morphological classification of bipolar cells of the primate retina. *European Journal of Neuroscience* **3**, 1069–1088.

CROOK, J.M., LANGE-MALECKI, B., LEE, B.B. & VALBERG, A. (1988). Visual resolution of macaque retinal ganglion cells. *Journal of Physiology* (London) **396**, 205–224.

DACEY, D.M. (1988). Dopamine-accumulating amacrine cells revealed by *in vitro* catecholamine-like fluorescence display a unique morphology. *Science* **240**, 1196-1198.

DACEY, D.M. (1989*a*). Axon-bearing amacrine cells of the macaque monkey retina. *Journal of Comparative Neurology* **284**, 275–293.

DACEY, D.M. (1989*b*). Monoamine-accumulating ganglion cell type of the cat's retina. *Journal of Comparative Neurology* **288**, 59–80.

DACEY, D.M. (1990*a*). The dopaminergic amacrine cell of the cat's retina. *Investigative Ophthalmology and Visual Science* (Suppl.) **31**, 535.

DACEY, D.M. (1990*b*). The dopaminergic amacrine cell. *Journal of Comparative Neurology* **301**, 461–489.

DACHEUX, R.F. & RAVIOLA, E. (1986). The rod pathway in the rabbit retina: A depolarizing bipolar and amacrine cell. *Journal of Neuroscience* **6**, 331–345.

DE MONASTERIO, F.M. & GOURAS, P. (1975). Functional properties of ganglion cells of the rhesus monkey retina. *Journal of Physiology* (London) **251**, 167–195.

FAMIGLIETTI, E.V. & KOLB, H. (1975). A bistratified amacrine cell and synaptic circuitry in the inner plexiform layer of the retina. *Brain Research* **84**, 293–300.

KAPLAN, E., LEE, B.B. & SHAPLEY, R.M. (1990). New views of primate retinal function. In *Progress in Retinal Research*, ed. OSBORNE, N. & CHADER, G., pp. 273–336. New York: Pergamon Press.

KAPLAN, E. & SHAPLEY, R.M. (1986). The primate retina contains two types of ganglion cells, with high and low contrast sensitivity. *Proceedings of the National Academy of Science of the U.S.A.* **83**, 2755–2757.

KOLB, H. & DEKORVER, L. (1991). Midget ganglion cells of the parafovea of the human retina: A study by electron microscopy of serial sections. *Journal of Comparative Neurology* **303**, 617–636.

LEVENTHAL, A.G., RODIECK, R.W. & DREHER, B. (1981). Retinal ganglion cell classes in the Old World monkey: Morphology and central projections. *Science* **213**, 1139–1142.

MARIANI, A.P. (1990). Amacrine cells of the rhesus monkey retina. *Journal of Comparative Neurology* **301**, 382–400.

MASTRONARDE, D.N. (1983). Interactions between ganglion cells in cat retina. *Journal of Neurophysiology* **49**, 350–365.

PEICHL, L. & WÄSSLE, H. (1983). The structural correlate of the receptive field centre of alpha ganglion cells in the cat retina. *Journal of Physiology* (London) **341**, 309–324.

PURPURA, K., KAPLAN, E. & SHAPLEY, R.M. (1988). Background light and the contrast gain of primate P and M retinal ganglion cells. *Proceedings of the National Academy of Science of the U.S.A.* **85**, 4534–4537.

RODIECK, R.W. (1988). The primate retina. In *Comparative Primate Biology. Neurosciences*, ed. STEKLIS, H.D. & ERWIN, J., pp. 203–278. New York: Alan R. Liss, Inc.

RODIECK, R.W., BINMOELLER, K.F. & DINEEN, J. (1985). Parasol and midget ganglion cells of the human retina. *Journal of Comparative Neurology* **233**, 115–132.

RODIECK, R.W. & HAUN, T.J. (1991). Parasol retinal ganglion cells in macaques connect intracellularly to other parasol cells, and to amacrine cells found in the ganglion cell layer. *Neuroscience Abstracts* **17**, 1375.

SAGAR, S.M. (1987). Somatostatin-like immunoreactive material in the rabbit retina: Immunohistochemical staining using monoclonal antibodies. *Journal of Comparative Neurology* **266**, 291–299.

SAGAR, S.M. & MARSHALL, P.E. (1988). Somatostatin-like immunoreactive material in associational ganglion cells of human retina. *Neuroscience* **27**, 507–516.

SHAPLEY, R. & PERRY, V.H. (1986). Cat and monkey retinal ganglion cells and their visual functional roles. *Trends in Neuroscience* **9**, 229–235.

SILVEIRA, L.C.L. & PERRY, V.H. (1991). The topography of magnocellular projecting ganglion cells (M-ganglion cells) in the primate retina. *Neuroscience* **40**, 217–237.

VANEY, D.I. (1991). Many diverse types of retinal neurons show tracer coupling when injected with biocytin or Neurobiotin. *Neuroscience Letters* **125**, 187–190.

VANEY, D.E., PEICHL, L. & BOYCOTT, B.B. (1988). Neurofibrillar long range amacrine cells in mammalian retinae. *Proceedings of the Royal Society B* (London) **235**, 203–219.

WÄSSLE, H. & BOYCOTT, B.B. (1991). Functional architecture of the mammalian retina. *Physiological Reviews* **71**, 447–480.

WÄSSLE, H. & CHUN, M.H. (1988). Dopaminergic and indoleamine-accumulating amacrine cells express GABA-like immunoreactivity in the cat retina. *Journal of Neuroscience* **8**, 3383–3394.

WÄSSLE, H., PEICHL, L. & BOYCOTT, B.B. (1981). Dendritic territories of cat retinal ganglion cells. *Nature* **292**, 344–345.

WÄSSLE, H., VOIGT, T. & PATEL, B. (1987). Morphological and immunocytochemical identification of indoleamine-accumulating neurons in the cat retina. *Journal of Neuroscience* **7**, 1574–1585.

WATANABE, M. & RODIECK, R.W. (1989). Parasol and midget ganglion cells of the primate retina. *Journal of Comparative Neurology* **289**, 434–454.

WHITE, C.A., CHALUPA, L.M., JOHNSON, D. & BRECHA, N.C. (1990). Somatostatin-immunoreactive cells in the adult cat retina. *Journal of Comparative Neurology* **293**, 134–150.